J Mol Model (2014) 20:2530
DOI 10.1007/s00894-014-2530-z

ORIGINAL PAPER

Combined effect of confinement and affinity of crowded environment on conformation switching of adenylate kinase

Min Li · Weixin Xu · John Z. H. Zhang · Fei Xia

Received: 24 August 2014 / Accepted: 12 November 2014 / Published online: 29 November 2014

Abstract The actual conformation switching of proteins in the crowded cellular environment is completely different from that in vitro. Proteins in cytoplasm are continually subject to confinement and/or attraction to other molecules in their surroundings due to the existence of various biological species. To gain insight into the nature of crowded environments, we investigated the effects of confinement and affinity on the conformation switching of adenylate kinase (ADK) in a spherical cavity. It was found that even a small degree of confinement reduces the entropy of the open state and stabilizes the closed state, which leads to increased energy barriers for transition. Furthermore, the analysis of transition temperatures and mean first passage times indicates that the proper affinity can promote the transition of ADK from closed state to open state. This study reveals that the crowded cellular environment plays an important role in the thermodynamics and kinetics of proteins in vivo.

Electronic supplementary material The online version of this article (doi:10.1007/s00894-014-2530-z) contains supplementary material, which is available to authorized users.

M. Li · J. Z. H. Zhang
State Key Laboratory of Precision Spectroscopy, Institute of Theoretical and Computational Science, East China Normal University, Shanghai 200062, China

W. Xu
Institute for Advanced Interdisciplinary Research, East China Normal University, Shanghai 200062, China

F. Xia (✉)
Department of Chemistry, East China Normal University, Shanghai 200062, China
e-mail: fxia@chem.ecnu.edu.cn

J. Z. H. Zhang (✉) · F. Xia
NYU-ECNU Center for Computational Chemistry at NYU Shanghai, Shanghai 200062, China
e-mail: john.zhang@nyu.edu

Keywords Confinement · Affinity · Crowded environment · Conformation switching · Adenylate kinase · 2D free energy profile

Introduction

How a protein accomplishes conformational transitions in the crowded cellular environment is a central issue in molecular biology [1]. Various kinds of macromolecules, such as ribosomes, RNAs and proteins, occupy approximately 30 % of the whole volume of cells [2–4]. No single macromolecule can be freely present at a high concentration of one species; instead, they all tend to get together to form a crowded environment in the cytoplasm, which is termed the excluded volume effect [5–8]. The high concentration of macromolecules in the cytoplasm has significant influence on biological processes, such as protein folding, genetic transcription, aggregation, and so on [9].

Aiming to explore the dynamic processes of macromolecules in crowded environments, a great deal of effort has gone into studies of confinement by means of various experimental techniques [10–13] and theoretical methods [9, 14–26]. Confinement involves the physical entrapment of the biomolecules concerned within rigid cavities of different sizes and shapes [16, 20, 25, 27, 28]. Biochemical experiments [10, 11] demonstrate that confinement enhances the thermodynamic stability of proteins in their native structure compared to that in dilute solution. However, some NMR studies [13, 29] found that in many cases of macromolecular crowding it is enthalpy rather than entropy that keeps proteins in unfolded states stable. On the other hand, theoretical studies [30, 31] reveal that confinement can stabilize the native structures of proteins and accelerate their folding process by reducing entropy. Further, Monte Carlo simulation [25] implies that a larger degree of confinement might have a destabilizing effect

on native structures, stemming from competition between entropic stabilization and enthalpic destabilization.

Molecular dynamics (MD) simulations based on all-atom models [23] can provide structural details of proteins at the atomic level, but it is difficult to reach the time scale of milliseconds required to study conformational switching. A useful physical model for the investigation of conformational transitions in proteins is the so-called Gō model that was proposed a decade ago [32, 33]. In the Gō model, every residue in a protein is represented by a coarse-grained bead, and the interactions of these beads are described by empirical potentials invented to emphasize native structures [32–35]. In an earlier version of the Gō model, interactions of the beads were described by simple attractive or repulsive non-bonded potentials [36]. The Gō model has been applied widely to study the kinetics of conformational change of proteins and has achieved numerous successes to date [33, 37]. Combined with confining potentials, it is now starting to be employed to explore the conformational switching of proteins in the crowded cellular environment. In most such studies, it is usual to construct a double-well Gō-like model [38] to gain information regarding intermediate states in the conformational transition for macromolecules such as RNA [37].

In this work, we investigated the conformational switching of adenylate kinase (ADK) in a crowded environment that was mimicked by confinement. ADK is an enzyme with 214 amino acid residues that plays an important role in the signal transduction process that catalyzes the conversion of adenosine triphosphate (ATP) to adenosine diphosphate (ADP) [39]. ADK is usually divided into three functional regions, namely, the LID domain (lid domain), the NMP domain (nucleotide monophosphate-bind domain) and the Core domain [39–41]. It is already known that ATP binds in the active pocket formed by the LID and Core domains, while ADP binds in the inactive pocket formed by the NMP and Core domains, with interconversion between the active (open) and active (closed) states [41]. In nature, ADK in the cytoplasm functions in a crowded environment as substrates bind to it. The crowded environment involves not only the spatial confinement formed by the immediate surroundings but also strong interactions with other macromolecules. It remains unclear how the conformational transition of ADK is affected by this complicated environment. In order to explore this, we placed a molecule of ADK in a spherical cavity, as shown in Fig. 1, to set up a model for MD simulations. Then, we investigated the effects of confinement and affinity on conformational switching of ADK.

The rest of paper is organized as follows: the following section on Theory and computational details gives the theoretical background and model parameters. The effects of temperatures, sizes of confining spheres and affinities on conformation switching of ADK are then discussed in the Results and discussion section, before summing up in Conclusions.

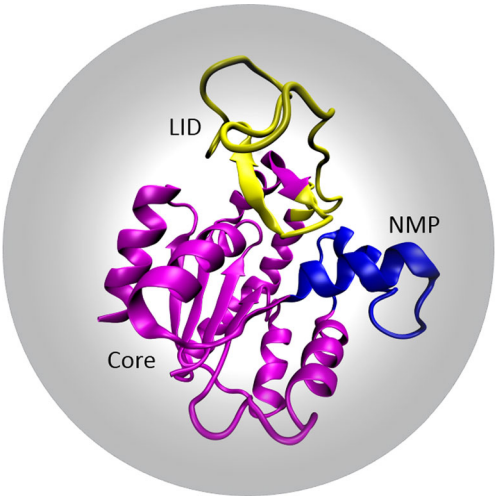

Fig. 1 Cartoon representation of adenylate kinase (ADK) in a spherical cavity. The LID, NMP and Core domains are highlighted in *yellow*, *blue* and *magenta*, respectively

Theory and computational details

Double-well Gō-like model

The double-well Gō-like model [42, 43] with the energy potential function U shown in Eq. (1) was used throughout our simulations. The energy function U explicitly includes the bond, bond-angle, torsion-angle and nonbonding interactions.

$$
\begin{aligned}
U(\Gamma,\Gamma_1,\Gamma_2) = & \\
& \sum_{bonds}^{N-1} K_b \qquad (b_i - b_{0i})^2 \\
& + \sum_{angles}^{N-2} K_\theta (\theta_i - \theta_{1i})^2 * (\theta_i - \theta_{2i})^2 \\
& + \sum_{dih}^{N-3} K_\varphi \left[\cos\left(\varphi_i - \frac{\varphi_{1i}+\varphi_{2i}}{2}\right) - \cos\left(\frac{\varphi_{1i}-\varphi_{2i}}{2}\right)\right]^2 \\
& + \sum_{|i-j|>3}^{nonnat} \varepsilon_0 \left(\frac{C}{r_{ij}}\right)^{12} + \sum_{|i-j|>3}^{nat} U_{nat}(r_{ij})
\end{aligned}
\tag{1}
$$

The conformation Γ is a function of Γ_1 and Γ_2, corresponding to the open and closed states of ADK. The first three terms describe the bond, angle vibration and dihedral rotation within adjacent four residues, where N is the total number of residues in protein. As described in our previous work [27, 28], the parameters b, θ, and Φ denote the virtual bond lengths, bond angles and dihedral angles, respectively. The parameter b_{0i} means the average values of bonds of both conformations Γ_1 and Γ_2. θ_{1i} (θ_{2i}) and φ_{1i} (φ_{2i}) stand for the corresponding

variables in the open (closed) structures. For the parameters K_b, K_θ and K_φ, the empirical values 100.0, 20.0 and 1.0 are adopted as previously reported [44, 45]. The fourth term describes nonnative interactions, where r_{ij} refers to the distance between the residues i and j, and ε_0 denotes a weight factor [27]. The parameter C [38, 42, 45] is always set as 4 Å to characterize the excluded volume repulsion between pairwise residues in the backbone.

The expression for the last native term U_{nat} [42] is shown in Eq.(2):

$$U_{nat}(r_{ij}) = \begin{cases} \varepsilon_1 Z(r)(Z(r)-2) \text{with } Z(r) = \left(\frac{r_1}{r}\right)^k \text{ if } r < r_1 \\ CY(r)^n \frac{\frac{Y(r)^n}{2} - (r_h - r_1)^{2n}}{2n} + \varepsilon_2 \text{with} \begin{cases} Y(r) = (r - r_h)^2 \\ C = \frac{4n(\varepsilon_1 + \varepsilon_h)}{(r_h - r_1)^{4n}} \end{cases} \text{if } r_1 \le r < r_h \\ -B\frac{Y(r) - h_1}{Y(r)^m + h_2} \text{with} \begin{cases} B = \varepsilon_1 m (r_2 - r_h)^{2(m-1)} \\ h_1 = \frac{\varepsilon_h (m-1)(r_2 - r_h)^2}{m(\varepsilon_2 + \varepsilon_h)} \\ h_2 = \frac{\varepsilon_2 (m-1)(r_2 - r_h)^{2m}}{\varepsilon_2 + \varepsilon_h} \end{cases} \text{if } r_h \le r < r_2 \\ \varepsilon_2 \left[5\left(\frac{r_2}{r}\right)^{12} - 6\left(\frac{r_2}{r}\right)^{10}\right] \text{if } r_2 \le r \end{cases} \quad (2)$$

where U_{nat} is a function of interacting distance r between two residues i and j. As shown in Fig. 2, r_1 is the position of first well while r_2 is that of the second. The term r_h represents the position of the transition state connecting the two wells; r_1 and r_2 denote the pairwise distances of residues in open and closed state, respectively. The value of r_h is set as $r_h=(r_1+r_2)/2$. Parameters m, k, and n are obtained by a smooth fit of the potential curve [42, 45]. The left well represents the open state of ADK and the right well represents the closed state. The

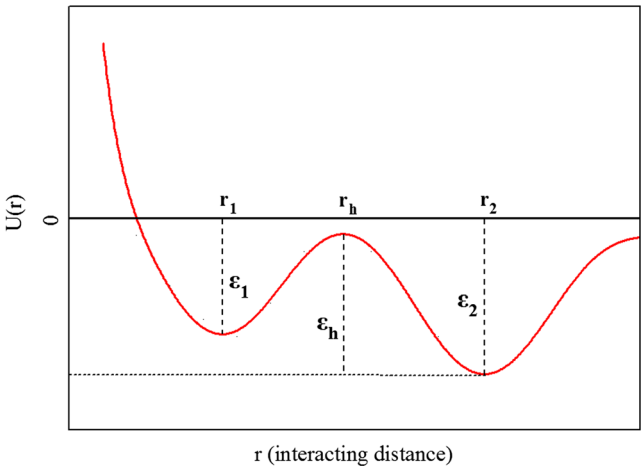

Fig. 2 A schematic illustration of the potential energy $U(r)$ of the double-well Gō-like model. The parameters r_1, r_2 and r_h denote the locations of the well of the open state, the well of the closed state and the transition state, respectively. The terms ε_1 and ε_2 describe the depths of wells of the open and closed states, respectively, while ε_h denotes the height of the barrier between the closed state and intermediate state

parameters ε_1 and ε_2 are the depths of the open and closed wells, respectively. The term ε_h denotes the height of the barrier from the closed well. In principle, the values of $\Delta\varepsilon=|\varepsilon_1-\varepsilon_2|$ and ε_h can be determined from experimental data. In practice, these two parameters were adjusted to achieve reasonable conformational switching between the open and closed states. In this study, the values of $\Delta\varepsilon$ and ε_h used were 1.1 and 1.2 kcal mol^{-1}, respectively.

Confining potentials

To mimic the effect of crowded environments, several different confining potentials, such as spherical potentials [25], cylindrical potentials [27], and planar potentials [22], have been used to model the confinement of limited spaces in cells. However, previous studies [22] have demonstrated that there is no substantial difference between spherical potentials and the others in accounting for crowed cellular environments. Thus, a spherical space was imposed on ADK throughout this work. In addition, another typical interaction term [26] shown in Eq. (3) was introduced into the total potential.

$$\sum_i^N \left[\left(\frac{C}{r_c - r_i}\right)^{12} - h\left(\frac{C}{r_c - r_i}\right)^6\right] \quad (3)$$

The term r_c denotes the radius of the confined sphere and r_i is the distance between a C^α atom and the center of the sphere. The parameter h denotes the affinity, and C is the same as in Eq. (1). Due to the hydrophobic and hydrophilic interactions in conformation transition, the two terms in Eq. (3) compromise the repulsive and attractive interactions between the surface of the sphere and all residues in the protein. The assigned 12-exponent repulsive potential introduces a repulsive boundary to avoid proteins approaching each other or coming out of the restricted space, while the 6-exponent attractive potential with affinity h dominates the interactions between the confined walls and residues of the protein. A larger value of h means stronger surroundings attracting ADK, while h=0 stands for no affinity at all. Since we are concerned with the influence of affinity on conformation switching, a series of values of h were applied in the Gō model and h-dependent folding dynamics were investigated.

Langevin dynamics simulations were performed according to Eq. (4) using a code implemented before, as described in previous work [27].

$$m\dot{v} = F(t) - \gamma v(t) + \Gamma(t) \quad (4)$$

In Eq. (4), t denotes the simulation time and the force $F(t)$ is calculated as the gradient of potential V according to $F(t)=$

$-\nabla V$, where the potential V includes all interactions in Eqs.1–3. The parameter γ is a viscosity constant set at $0.05\tau^{-1}$, and τ is the time unit of period of oscillations. To be consistent with the reduced units, we set the value of the viscosity constant γ as 0.25 in this study. The velocity $v(t)$ in the second term was derived from the second derivative of the total potential V, which contains the effects of confinement and affinity. The last term Γ represents random force [28].

Model setup and parameters

The crystal structures with PDB IDs 1ANK and 4AKE were downloaded from the PDB bank (http://www.rcsb.org). Only the Cα atoms of A chains in 1ANK and 4AKE were chosen for constructing the native open and closed states in the double-well Gō model. Langevin dynamics simulations were then carried out at different conditions of temperature (0.5–1.05), radii (5–40 Å) and affinities (0.0–2.0) starting from the closed state of ADK to sample the transition ensembles, until ADK reached a stable open state [46–48]. Finally, the simulated trajectories were analyzed and plotted. In addition, the exponential functions were used to fit the data of T_f in Fig. 6 to obtain smooth curves. To analyze the residue interactions in closed and open states of ADK, residue pairs within a cut-off value of 4.5 Å were defined to form "native contacts".

Results and discussion

Transition ensembles of ADK in bulk

To estimate the effect of different temperatures on the conformational switching of ADK, four simulations starting from the closed states were performed at temperatures T=0.5, 0.65, 0.75 and 0.95 (Supporting Information, Fig. S1), respectively. At the lower temperatures of 0.5 and 0.65, ADK could not break the native contacts in closed state and had a lower probability to switch to the open state. As the temperature increased up to 0.75, i.e., around the transition temperature T_f^0=0.78 [49], ADK could reside in the open state and closed state with equal probability, switching rapidly between the closed and open states. At the high temperature (0.95), many native contacts in ADK broke and resulted in unstable conformations. The calculated values of root mean squared deviation (RMSD) of both open and closed states are larger than those at low temperatures. The features of conformation transitions of ADK at different temperatures could also be characterized by the constructed two dimensional (2D) free energy profiles (Supporting Information, Fig. S2).

We evaluated the population rates of closed and open states of ADK at different temperatures and obtained a value of transition temperature T_f = 0.78 using a linear fitting [42]. The typical transition pathways [38, 45] of ADK from the closed state to open state near T_f in bulk are displayed in Fig. 3a. The constructed free energy profiles show that the barrier from the closed state to the intermediate is much higher than that from the intermediate to the open state, which indicates that the transition from the closed state to the intermediate state is the rate determining step for the whole transition process. The secondary structures obtained by cluster analysis at the temperature T=0.80 shown in Fig. 3b reveal that the LID domain of ADK first dissociates to form an intermediate state, followed by movement of the NMP domain, which is in good agreement with previous findings that conformation switching of ADK travels mainly along the NMP-closing pathway [45].

Confinement at different radii

In order to explore the confinement effect without affinity, the 2D free energy profiles of conformation transitions at different radii were plotted (Fig. 4). The energy profile of ADK in bulk (Fig. 4a) was taken as a reference for conformational

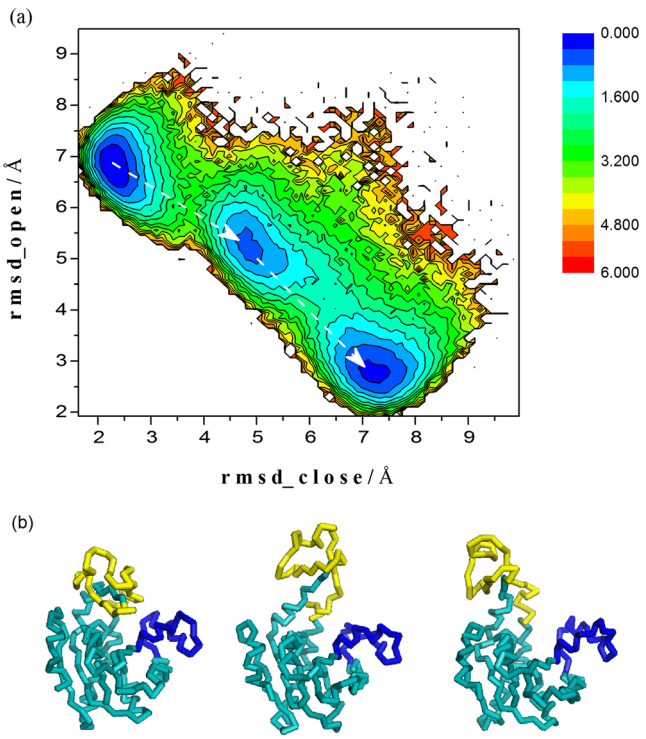

Fig. 3 **a** Two-dimensional (2D) free energy profile at temperature T=0.80 in bulk as a function of the root mean square deviations (RMSD) of closed and open states, denoted as rmsd_close and rmsd_open (in Ångstroms). *White arrows* Transition paths from the closed state to open state through the intermediate state. The free energies range from 0.0 to 6.0 and in the unit of $K_BT_f^0$. **b** Ribbon representations of the backbones of three structures corresponding to the three minima of closed, intermediate and open states in **a**. *Blue*, *yellow* and *green* regions denote the key NMP, LID and Core domains of ADK, respectively

switching without confinement. When the radii of confined spheres take the values 5 Å or 9.5 Å, the constructed contour maps of free energies in Fig. 4b and c are extremely abnormal since the sampled structures of ADK in trajectories distort drastically from the native structures. As the radius adopts 12 Å, the volume is sufficient for ADK to make a successful conformational transition through space. Figure 4 reveals that confinement within spherical walls can prevent ADK from switching. That means that proteins immersed in cytoplasm can be repelled by surrounded biomolecules so that their conformational switching might be hampered or even fail because of too crowded surroundings. Within a larger space, the confinement of environment has less effect on ADK conformational switching and the dynamic behavior of ADK is similar to that in bulk.

Affinity effect

In vivo, the interactions between embraced proteins and their surroundings are very complicated, and involve strong repulsive and attractive interactions. This section focuses on exploring the effect of affinity on the ADK transition within a confined cavity. Based on the results in Fig. 4, the radius of the sphere was fixed at 12 Å, which allows ADK to switch to the open state; meanwhile, the parameter h of affinity adopts a series of values that correspond to different strengths caused by the surroundings.

The plots in Fig. 5 clearly show that the different affinities do influence the conformational switching of ADK at the temperatures chosen. Even at the low temperature T=0.5, the strong affinity h=1.5 still has a considerable impact on the switching process, as shown in Fig. 5g. Comparing the contours of 2D free energy profiles at the affinities 0.5, 1.0 and 1.5 indicates that the conformational spaces of the intermediate and open states are visited more frequently, with larger affinities at the same temperatures. This means that the strong attractions between proteins in crowded environments could make the native contacts in proteins break more easily, effectively facilitating their transition processes. The conformational spaces have been referred to as multiple long and broad valleys [42] on the landscapes of transition that could be visited by ADK with the help of strong affinities, as shown in Fig. 5g–i. In other words, the attractive interactions actually accelerate conformation switching of proteins in crowded environments to some extent.

In addition, another basin has been mentioned to be located near the native structure of the closed state in Fig. 5f, but obviously this does not connect the intermediate state as well as the open state with the available transition pathways. The existence of such a basin could be explained readily by the funnel energy landscape theory [50–53]. Since the energy landscape is fairly rugged, the ADK might be trapped in a certain energy minimum near the closed state under high enthalpic and entropic conditions. Each temperature is associated with an optimal affinity with which the closed state transits to the open state most quickly. It is clear that the conformation switching of protein in crowded environments needs to be properly governed and regulated by cells in order to carry out their wide range of physiological activities.

T_f and mean first passage time analysis

To further confirm the significant effects of confinement and affinity, we explored the relationship between T_f and radius

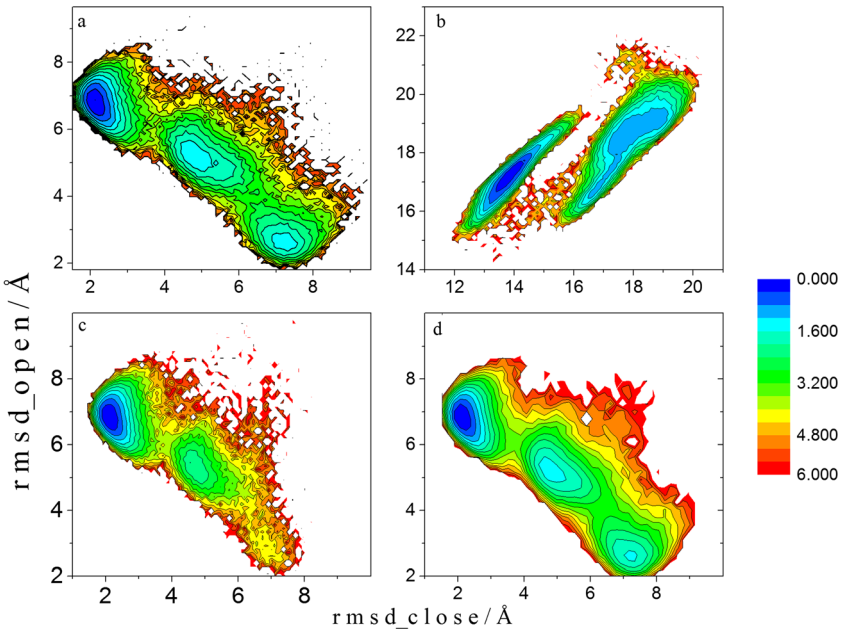

Fig. 4 The 2D free energy profiles **a** in bulk and **b**–**d** at different radii (**b** R= 5.0, **c** R= 9.5, **d** R= 12 Å) without affinity at T=0.75, as a function of the calculated rmsd_close and rmsd_open in Ångstroms. The values of free energies range from 0.0 to 6.0 in units of $K_B T_f^0$

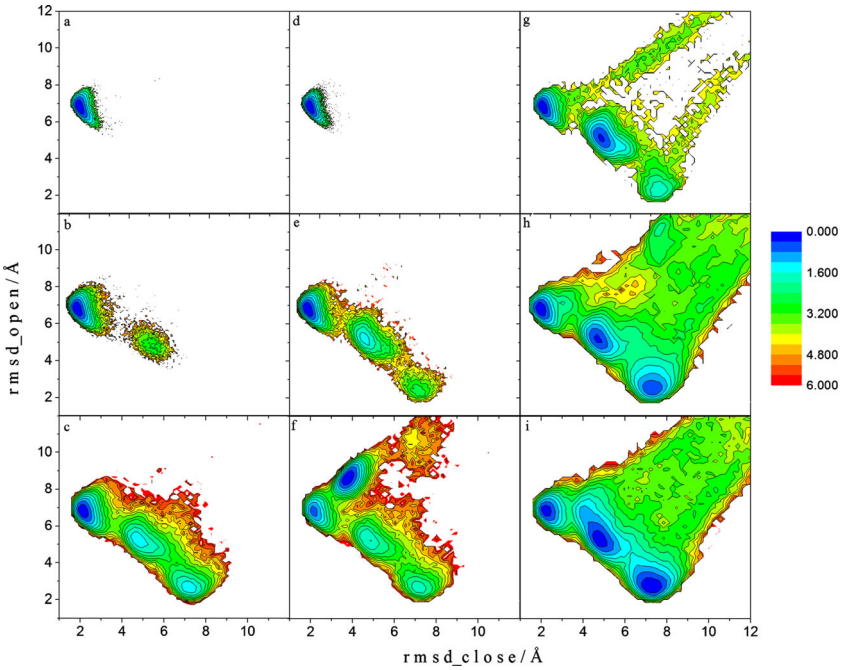

Fig. 5 **a**–**c** The 2D free energy profiles with affinity h=0.50 (**a**, **d**, **g**), h=1.0 (**b**, **e**, **h**), and h=1.5 (**c**, **f**, **i**) at different temperatures [T=0.50 (**a**–**c**), 0.65 (**d**–**f**) or 0.75 (**g**–**i**)] as a function of the calculated rmsd_close and rmsd_open in Ångstroms. The radii of spherical cavities in all simulations was fixed at 12 Å. The values of free energies range from 0.0 to 6.0 in units of $K_BT_f^0$

and estimated the transition rates of ADK by using the mean first passage time (MFPT) [42]. Figure 6a shows the data of T_f varying with the radius R. Previous studies [22, 25] reported that the calculated difference of T_f–T_f^0 is proportional to the function $R^{-\gamma}$, in which the parameter γ depends on specific ensembles. In this work, we fitted the data of T_f using an exponential function with γ=3.75 (see Supporting Information, Fig. S4). The smooth curve obtained in Fig. 6a indicates that T_f appears to decay exponentially with increasing radii, which suggests that confinement is a local effect dependent on T_f. It should be noted that, below 12 Å, the conformational switching always needs higher T_f, while beyond 12 Å the T_f

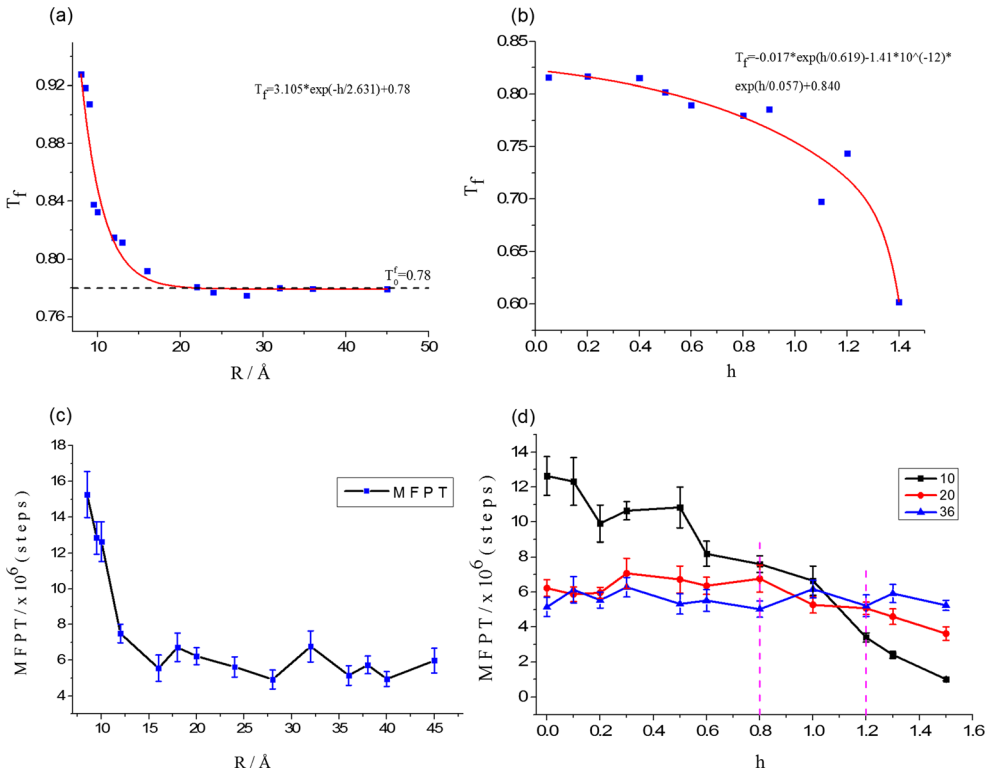

Fig. 6 **a**, **b** Plots of T_f changing with radius R and affinity h, respectively. T_f data in **a** and **b** are fitted with *red curves* using the exponential functions shown. The *dashed line* in **a** represents the value T_f=0.78 in bulk. **c**, **d** Mean first passage time (MFPT) changes with R and h, respectively. In **d**, the *black*, *red* and *blue curves* denote the data obtained at R=10, 20 and 36 Å, respectively. Calculated *error bars* mean standard deviations of MFPT values

remains almost invariant around 0.78. The variation tendency of T_f indicates that the crowded environment has no substantial effect on conformational switching of ADK if the radii of the confined spheres are larger than 12 Å.

Figure 6b also shows the dependence of T_f on different affinity values. An exponential fit of T_f data shows that the change in T_f is very small when *h* is within 0.8. Compared to the T_f=0.78 of ADK in bulk, it seems that interactions with low affinities are less helpful in breaking residue contacts in ADK so that the affinity effects are not remarkable and are similar to those in bulk. Nevertheless, T_f drops dramatically to 0.6 as *h* increases to 1.4, which demonstrates that strongly crowded environments affect T_f considerably. Besides, it was noted that ADK trapped in excessively small spaces could not undergo switching, and the exact biological cavities in cells should be of a suitable size for the accommodation of proteins.

Figure 6c shows that the calculated MFPT values vary linearly with radii where R is less than 12 Å, which is consistent with a previous study by Nitin et al. [25]. Beyond 12 Å, MFPT values fluctuate around 6.0, which implies that spatial confinement is not the crucial factor impacting on switching rates at large distances. The results in Fig. 6d indicate that the switching rates can be enhanced greatly by changing the radii and affinity strengths. When the radii of confinement spheres are much larger than the size of native states of ADK, the transition rates do not change markedly and are similar to those in bulk. When R adopts a suitable value such as 10 Å, the MFPT values exhibit a clear dependence on the increasing affinity values.

Free energy barriers

Another concern about confinement is how it influences the transition pathways of ADK. Figure 7a displays the one-dimensional energy profiles projected from the 2D free energy profiles, and shows that the open states become apparently less stable in energy when R becomes smaller, as indicated by the dashed curve ΔG_O. The reason for this lies in the fact that

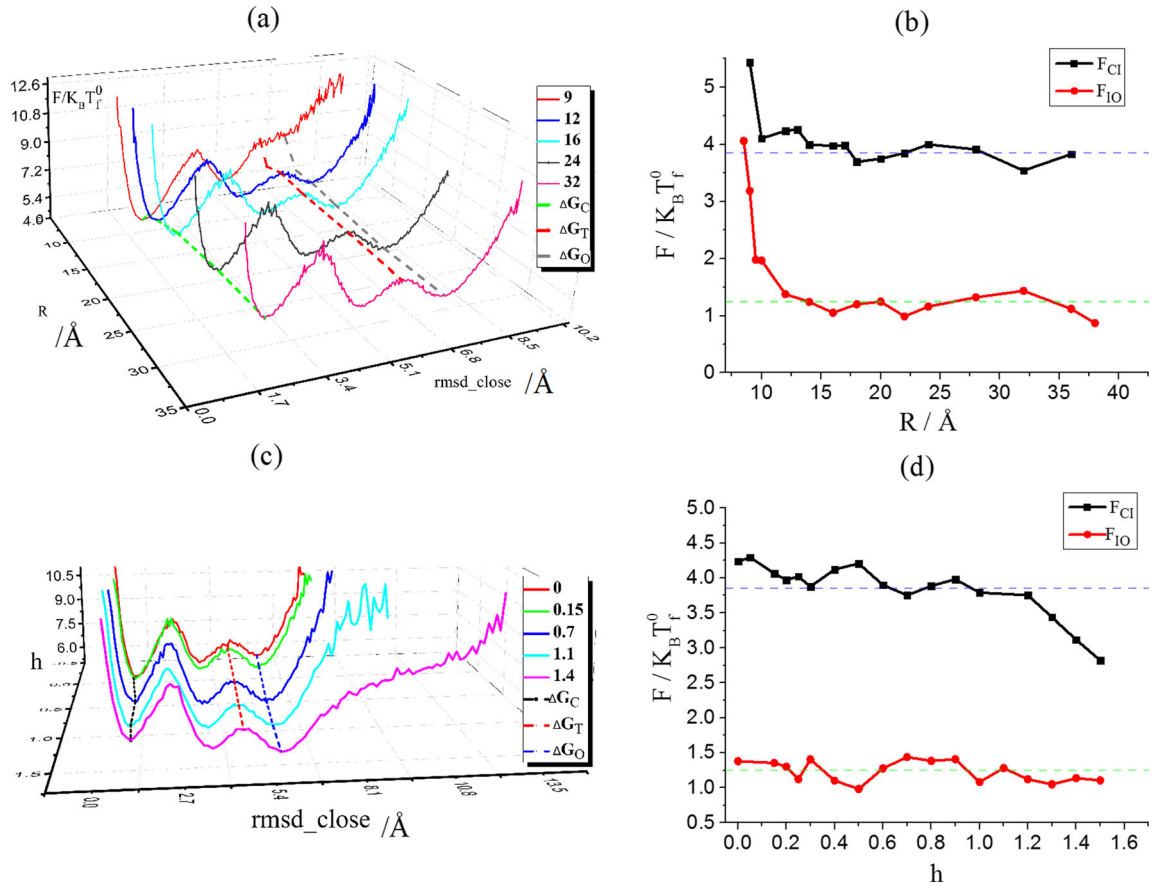

Fig. 7 **a** One-dimensional free energy profiles as functions of the radius R and rmsd_close (Ångstroms). *Red*, *blue*, *cyan*, *dark* and *pink* curves represent R=9, 12, 16, 24 and 32 Å, respectively. *Green*, *red* and *gray dashed curves* show the connections of free energy values of the closed states, second transition states and open states, denoted by ΔG_C, ΔG_T and ΔG_O, respectively. **b** Evaluated values of free energy heights at different R (Ångstroms). F_{CI} and F_{IO} denote barriers from the closed state to an intermediate state and from intermediate to open state, respectively. **c** One-dimensional free energy profiles as functions of the affinity *h* and rmsd_close (Ångstroms). *Red*, *green*, *blue*, *cyan* and *magenta* curves represent *h*=0, 0.15, 0.7, 1.1 and 1.4, respectively. *Black*, *red* and *blue dashed* curves show the connections of free energy values of the closed states, the second transition states and open states, defined by ΔG_C, ΔG_T and ΔG_O, respectively. **d** Calculated values of free energy heights at different *h*. F_{CI} and F_{IO} are the same as in **b**. The free energies F in all plots are in units of $K_BT_f^0$

confinement destabilizes the open state by reducing entropies and thus makes a significant contribution to the stabilization of closed states. The results in Fig. 7b indicate that both the calculated barriers F_{CI} and F_{IO} become higher with smaller R values. The first barrier F_{CI} is larger than the second F_{IO} by 2.5 $K_BT_f^0$. thus ADK prefers the closed state under compact confinement and it is difficult to transit to the open state [22].

Figure 7c shows the variations in free energy profiles with affinity *h* at a fixed R. It can be seen that the weak affinities with $h<1.0$ almost do not change the free energy profiles at all. However, the strong attractions seen at $h>1.0$ can effectively facilitate ADK to switch to the open states The energy profile at $h=1.4$ shows that the energy well of the open state is lower than that of the corresponding intermediate state and closed state, which could be attributed to the enthalpic stabilization generated by affinity. A strong affinity could promote the escape of ADK from the closed well and keep it stable in an open state. The calculated

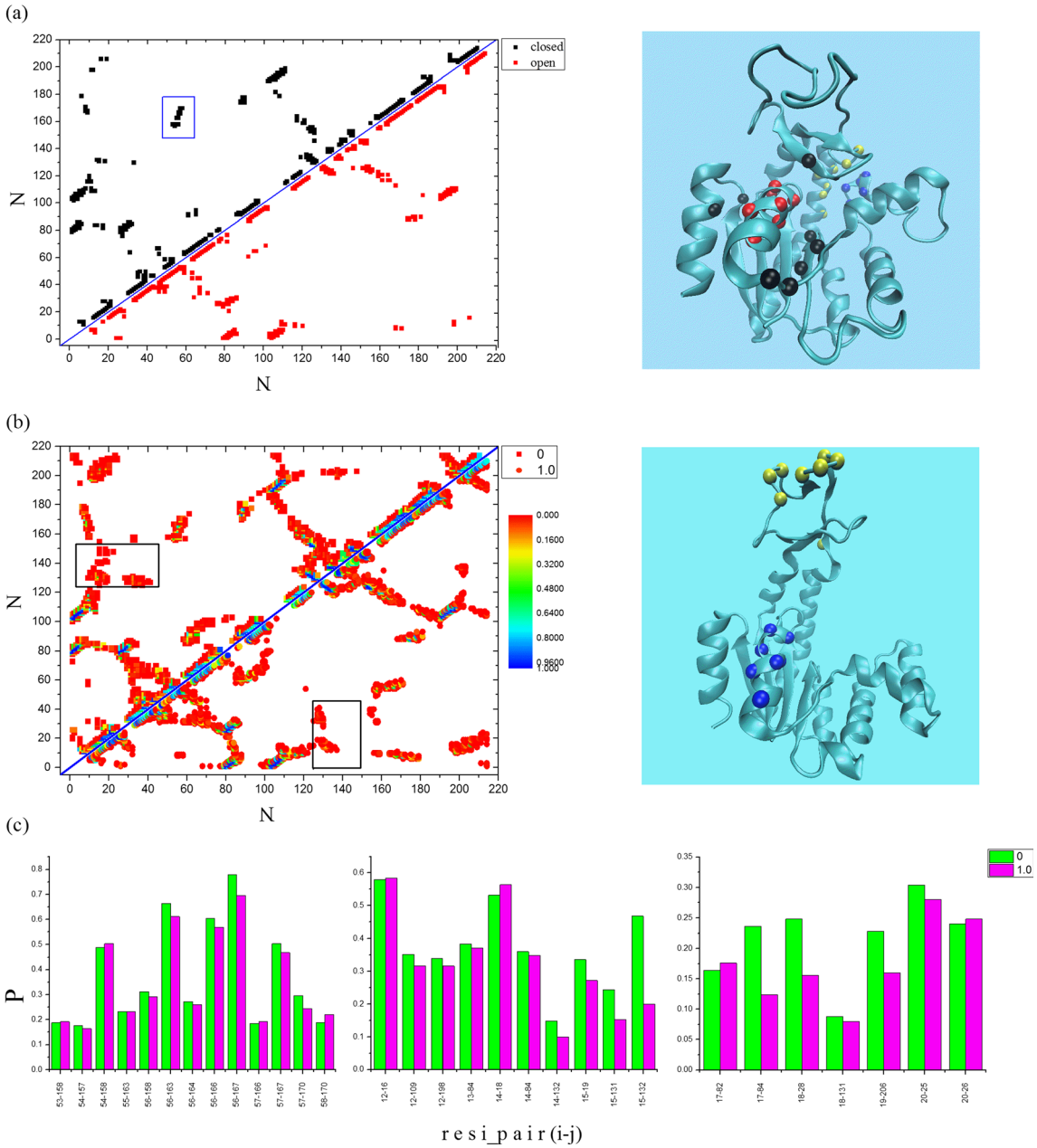

Fig. 8 **a** *Left* Comparison of residue interactions between the closed and open states of ADK with respect to the residue index N. The area of greatest difference between two states is highlighted in a *blue square*. *Right* Typical structure of the closed state; *blue*, *yellow*, *red* and *black beads* denote residues crucial to stabilization of interactions between LID, NMP and Core domains. **b** *Left* Constructed contact map at $h=0.0$ and 1.0. *Black squares* highlight the areas of greatest difference between the two sets of data. *Right* Structure of the open state, where the contact interactions of the *yellow* and *blue beads* are crucial for conformation transition. **c** Comparison of probability distributions, *P*, of the native contacts with respect to the residue pairs *i* and *j*, based on the trajectories obtained at $h=0.0$ and 1.0

values of the first barrier F_{CI} in Fig. 7d appear to be more sensitive than F_{IO} to the affinity h, especial for values larger than 1.0. Although the energy difference between barriers is approximately 2.5 $K_B T_f^0$. the wells of both intermediate and open states are much deeper than the closed states under this strong attraction. The results further prove that affinity effects of the environment play an important role in changing the kinetics of conformational switching of ADK.

Contact maps

A detailed comparison of native contacts between the closed and open states of ADK is shown in Fig. 8a. The major difference between the open and closed states lies in the regions of the LID and NMP domains, where native contacts might be formed in the closed state but not in the open state, such as residues 53–58 in the NMP domain and 163–170 in the LID domain, highlighted by the blue square in the left plot in Fig. 8a. As shown in the right structure of the closed state, the residue pairs G14-V132, T15-R131 and T15-V132 are of great importance for Core/LID binding [38], while the Core domain stabilizes the closed structure by forming contacts between helical residues 12–20 and the surrounding residues, as indicated by the red and black beads. During conformational switching, these contacts in the LID and NMP domains would break to facilitate the transition process.

Figure 8b shows the analysis of contacts of residue pairs under confinement with or without affinity. The major differences under confinement with h=0 and 1.0 are marked with black squares. In the crowded environment, ADK forms many pairwise residue contacts between the loop of the LID and the helix of the Core during the transition. If the affinity is strong enough, the LID region would move away from the Core domain. The right structure shows that some residue contacts are deconstructed under the affinity of h=1.0 compared to h=0.0, such as the yellow beads 140–150 in LID and blue beads 14–19 in the Core domain. The probability distributions of native contacts of key residue pairs in the transition are further calculated in Fig. 8c. The left, middle and right plots present the crucial pairwise residue interactions in different regions. A comparison of three histograms indicates that the affinity strongly affects the contact interactions of residue pairs such as T15-R131, T15-V132 in the Core/LID domains and A17-D84, Q18-Q28, F19-R206 in the Core domain. Affinity favors dissociation of LID domain from the Core domain by breaking the pairwise contacts T15-R131 and T15-V132, which lowers the first barrier and changes the kinetics of the NMP-closing pathway.

Conclusions

The Gō-like double-well model was employed to investigate conformational switching of ADK under confinement and affinity in a crowded environment. We explored the transition processes of ADK in bulk, with affinity and without affinity, respectively. Interestingly, we found that, compared to the transition of ADK in bulk, confinement indeed makes a significant contribution to the stabilization of closed states. The influence of confinement on T_f is quite remarkable within a distance 12 Å; beyond that the conformational switching of ADK is similar to that in bulk. It was also noted that an extremely small degree of confinement completely prevents ADK from switching from closed state to open state due to the steric effect. In contrast, the affinity facilitates the conformational switching of ADK from closed states by stabilizing the open states. The simulation results demonstrate that strong affinities with h>1.0 drastically enhance the transition rates of ADK. It can be concluded that the affinity of the environment has an effect on the conformation switching of proteins only if they are within a valid distance. Based on our simulations, the effect on proteins of confinement and affinity of the crowded environment in cells can be understood clearly. Significantly, our results reveal that the conformation switching of proteins occurring in cells is actually affected by the combined effect of confinement and affinity of surroundings, which is distinctively different from that in bulk.

Acknowledgments This work was supported by the National Natural Science Foundation of China (Grants No. 21433004 and 21473056), Shanghai Pu Jiang Program (12PJ1403000), Shanghai Natural Science Foundation (14ZR1411800) and a start-up grant of ECNU (41500-515430-14100/001/136). We also thank the supercomputer center of ECNU for computer time.

References

1. Ellis R (2001) J Curr Opin Struct Biol 11:500
2. Minton AP (2005) J Pharm Sci 94:1668
3. Ellis RJ, Minton AP (2003) Nature 425:27
4. Minton AP (2001) J Biol Chem 276:10577
5. Minton AP (1983) Mol Cell Biochem 55:119
6. Minton AP (1998) Methods Enzymol 295:127
7. Zimmerman SB, Minton AP (1993) Annu Rev Biophys Biomol Struct 22:27
8. Zimmerman SB, Trach SO (1991) J Mol Biol 222:599
9. Friedel M, Sheeler DJ, Shea JE (2003) J Chem Phys 118:8106
10. Eggers DK, Valentine JS (2001) Protein Sci 10:250
11. Eggers DK, Valentine JS (2001) J Mol Biol 314:911
12. Lei C, Shin Y, Liu J, Ackerman EJ (2002) J Am Chem Soc 124: 11242
13. Wang YQ, Sarkar M, Smith AE, Krois AS, Pielak GJ (2012) J Am Chem Soc 134:16614
14. Arkin H, Janke W (2012) J Phys Chem B 116:10379
15. Chen E, Christiansen A, Wang Q, Cheung MS, Kliger DS, Wittung-Stafshede P (2012) Biochemistry 51:9836

16. Klimov DK, Newfield D, Thirumalai D (2002) Proc Natl Acad Sci USA 99:8019
17. Kurniawan NA, Enemark S, Rajagopalan R (2012) J Am Chem Soc 134:10200
18. Lucent D, Vishal V, Pande VS (2007) Proc Natl Acad Sci USA 104: 10430
19. Malik A, Kundu J, Mukherjee SK, Chowdhury PK (2012) J Phys Chem B 116:12895
20. Marino KA, Bolhuis PG (2012) J Phys Chem B 116:11872
21. Martin J (2004) J Mol Recognit 17:465
22. Mittal J, Best RB (2008) Proc Natl Acad Sci USA 105:20233
23. Predeus AV, Gul S, Gopal SM, Feig M (2012) J Phys Chem B 116: 8610
24. Rao JS, Cruz L (2013) J Phys Chem B 117:3707
25. Rathore N, Knotts TA, de Pablo J (2006) J Biophys J 90:1767
26. Wojciehowski M, Cieplak M (2008) Biosystems 94:248
27. Xu WX, Wang J, Wang W (2005) Proteins 61:777
28. Wang W, Xu WX, Levy Y, Trizac E, Wolynes PG (2009) Proc Natl Acad Sci USA 106:5517
29. Benton LA, Smith AE, Young GB, Pielak G (2012) J Biochem 51: 9773
30. Zhou HX (2004) J Mol Recognit 17:368
31. Zhou HX, Dill KA (2001) Biochemistry 40:11289
32. Nakamura HK, Sasai M, Takano M (2004) Chem Phys 307:259
33. Cieplak M, Hoang TX, Robbins MO (2002) Proteins 49:114
34. Hayward S, Go N (1995) Annu Rev Phys Chem 46:223
35. Kim J, Keyes T (2008) J Phys Chem B 112:954
36. Ueeda Y, Taketomi H, Go N (1978) Bioplymers 17:1531
37. Hills RD, Brooks CL (2009) Int J Mol Sci 10:889
38. Lu Q, Wang J (2008) J Am Chem Soc 130:4772
39. Whitford PC, Miyashita O, Levy Y, Onuchic JN (2007) J Mol Biol 366:1661
40. Daily MD, Phillips GN, Cui QA (2010) J Mol Biol 400:618
41. Beckstein O, Denning EJ, Perilla JR, Woolf TB (2009) J Mol Biol 394:160
42. Lai ZZ, Lu Q, Wang J (2011) J Phys Chem B 115:4147
43. Chu JW, Voth GA (2007) Biophys J 93:3860
44. Levy Y, Wolynes PG, Onuchic JN (2004) Proc Natl Acad Sci USA 101:511
45. Lu Q, Wang J (2009) J Phys Chem B 113:1517
46. Cellmer T, Bratko D, Blanch H (2003) Biophys J 84:41a
47. Dukovski I, Muthukumar M (2003) J Chem Phys 118:6648
48. Liu C, Muthukumar M (1998) J Chem Phys 109:2536
49. Clementi C, Nymeyer H, Onuchic JN (2000) J Mol Biol 298:937
50. Bryngelson JD, Onuchic JN, Socci ND, Wolynes PG (1995) Proteins 21:167
51. Dill KA, Chan HS (1997) Nat Struct Biol 4:10
52. Onuchic JN, LutheySchulten Z, Wolynes PG (1997) Annu Rev Phys Chem 48:545
53. Wolynes PG (2005) Philos T R Soc A 363:453